DOI: 10.1002/(( ))
Article type: Communication

Isomer-pure bis-PCBM assisted crystal engineering of perovskite solar cells showing excellent efficiency and stability

Fei Zhang, Wenda Shi, Jingshan Luo, Norman Pellet , Chenyi Yi, Xiong Li, Xiaoming Zhao, T. John. S. Dennis, Xianggao Li, Shirong Wang*, Shaik Mohammed Zakeeruddin, Dongqin Bi*, Michael Grätzel**

F. Zhang, X. Zhao, Prof. X. Li, Prof. S. Wang*
School of Chemical Engineering and Technology, Tianjin University
300072 Tianjin, China
Email: wangshirong@tju.edu.cn

F. Zhang, Dr. J. Luo, N.Pellet, Dr. C. Yi,Dr. X. Li, Dr. S. M. Zakeeruddin, Dr. D. Bi *, Prof. M. Grätzel*
Laboratory of Photonics and Interfaces, Institute of Chemical Sciences and Engineering,
École Polytechnique Fédérale de Lausanne (EPFL)
Station 6 CH-1015, Lausanne, Switzerland
Email: dongqin.bi@epfl.ch ; michael.graetzel@epfl.ch

F. Zhang, X. Zhao, Prof. X. G. Li, Prof. S. Wang*
Collaborative Innovation Center of Chemical Science and Engineering(Tianjin)
300072 Tianjin, China

W. Shi, X. Zhao, Dr. T. J. S. Dennis*
School of Physics and Astronomy, Queen Mary University of London,
327 Mile End RoadLondon, E1 4NS, UK
Email: j.dennis@qmul.ac.uk

Keywords: stability; PCBM; perovskite solar cell;bis-PCBM

Abstract: We prepared the novel fullerene derivative (α-bis-PCBM) by separating it from the as-produced bis- phenyl-C_{61}-butyric acid methyl (bis-[60] PCBM) ester isomer mixture using preparative peak-recycling high performance liquid chromatography (HPLC). We employed the compound as a templating agent for the solution processing of metal halide perovskite films by the antisolvent method. Perovskite solar cells (PSCs) containing α-bis-PCBM perovskite achieve better stability, efficiency, and reproducibility compared with those employing traditional PCBM. The α-bis-PCBM can fill the vacancies and grain boundaries of the perovskite film, enhancing the crystallization of perovskites and addressing the issue of

slow electron extraction. In addition, it can also resist the ingression of moisture, protect the interfaces from chemical erosion, and passivate the voids or pinholes generated in the hole-transporting layer. As a result, we obtain an outstanding power conversion efficiency (PCE) of 20.8 % compared with 19.9 % by PCBM, accompanied by excellent stability under heat and simulated sunlight,. The PCE of unsealed devcies dropped by less than 10% in ambient air (40% RH) after 44 days at 65 ℃ and by 4% after 600 h under continuous full sun illumination and maximum power point tracking respectively.

Hybrid organic-inorganic lead halide perovskite solar cells (PSCs) have emerged as a promising candidate for the next generation photovoltaic technology due to their low manufacturing cost and high performance.[1–6] Through judicious manipulation of perovskite morphology and improvement of interfacial properties,[2–6] PSCs have reached a certified power conversion efficiency (PCE) up to 22.1%.[7] Generally, the PSCs with the best performance employ a sandwich configuration, composed of a layer of TiO_2 electron selective contact, which is infiltrated by the intrinsic perovskite light harvester, followed by a layer of hole transport material (HTM) as p-type contact and a metal back contact.[8]

Despite of these stunning advances, several challenges still remain before PSCs become a competitive commercial technology, one crucial issue being the device stability.[9–11] Uncontrolled film morphology associated with poor crystallity of the perovskites results in low efficiency and poor reproducibility of the device performance.[12] Previous studies have indicated that the degradation of PSCs is primarily governed by the ingress of atmospheric oxygen and water vapor into the film upon exposure to air, which in turn causes undesired reactions with the active materials.[13,14] Various methods have been tried to modify the morphology of perovskite films aiming to improve the stability, for example, poly(methyl methacrylate) (PMMA) was used as a template to control nucleation and crystal growth, resulting in considerable increase in both the device efficiency and stability when kept under

dry condition in the dark. [15] Other studies use additives like 1-methyl-3-(1H,1H,2H,2H-nonafluorohexyl)-imidazolium iodide,[16] or phenyl-C_{61}-butyric acid methyl ester (PCBM)[17-19] or alkali metal ions [20] in the pervokite precursor solution film to improve film formation and increase the environmental stability. However, very few investigations achieve stability under both prolonged heat and light soaking stress with PSCs exhibiting a high PCE and good moisture resistance.[21]

A bis-analogue of PCBM, bis-PCBM, was successfully utilized in polymer solar cells to improve the open-circuit voltage (V_{oc}) over simple PCBM.[22,23] However, the increase in PCE is not as high as expected from the increase in $V_{OC,}$ which is because that bis-PCBM exists as a mixture of 19 structural isomers, which leads to morphological and energetic disorder in the active layer of photovoltaic devices, resulting in a degrading effect on the J_{sc} [24]. The disorders induced by the isomer mixture may be removed through fabricating devices from isomer-pure samples. Hence, using isomer-pure samples may potentially lead to both higher voltage and higher current in the polymer solar cells, compared to the isomer mixture.[25]

Herein, we report on the separation isolation of the pure α–bis-PCBM isomer from the reaction mixture of isomers by preparative peak-recycling high performance liquid chromatography (HPLC). We employ it as a templating agent in the chlorobenzene antisolvent to enhance the electronic quality and PV performance of solution processed perovskite films. Our results show that the α–bis-PCBM leads to (i) enlargement of the perovskite grain size, (ii) passivation of the interface trap states at the grain boundaries, and (iii) improvement of the charge carrier separation and transportation within the perovskite film.[26-28] As a result, the newly developed PSCs using α–bis-PCBM as an additive in the antisolvent to template the nucleation and growth of the PSC attain a PCE of 20.8 %, compared with 18.8 % for the PCBM-free reference and 19.9 % for PCBM itself- Importantly this PCE increase comes along with enhanced stability under heat and illumination.

Figure 1 shows a schematic illustration of the α–bis-PCBM or PCBM-assisted growth process for the perovskite- α–bis-PCBM or PCBM layer. We produce the mixed cation perovskite $[(FAI)_{0.81}(PbI_2)_{0.85}(MABr)_{0.15}(PbBr_2)_{0.15}]$ films in a single step from a solution of formamidinium iodide (FAI), PbI_2, methylammonium bromide (MABr) and $PbBr_2$ in a mixed solvent of dimethyl formamide (DMF) and dimethyl sulfoxide (DMSO). The perovskite spin-coating procedure employed 2000 rpm for 10 s followed by 6000 rpm for 30 s. During the last 15 s of second spin coating step 100 ml of α–bis-PCBM containing chlorobenzene (CB) was dropped onto the above film to template the nucleation and growth of the perovskite crystals.

Figure S2 shows the scanning electron microscopy (SEM) images of corresponding perovskite films deposited on m-TiO_2/c-TiO_2/FTO substrate. As illustrated from the top-view SEM, the grain size of the perovskite film increases with the use of PCBM / α–bis-PCBM and directs most of the grain boundaries to assume a perpendicular orientation to the substrate. Hence, the PCBM or α–bis-PCBM is expected to uniformly trigger heterogeneous nucleation over the perovskite precursor film, improving the grain size and facilitating the perovskite to grow in preferred direction. Reflections of facets with (111) indices become dominant because of the low symmetry of the trigonal perovskite (p3m1) phase as indicated in the XRD pattern in **Figure 2a**.[15] Whereas the cross-sectional SEM of the reference film reveals numerous grain boundaries, very few appear in the PCBM or α–bis-PCBM-containing film. The high-angle annular dark-field scanning transmission electron microscopy (HAADF-STEM) indicates that the α–bis-PCBM can fill in the vacancies and grain boundaries of the perovskite film(**Figure S3)**.We also measured the contact angle between the corresponding films and CB and present the results in **Figure S4**. The angle of a CB droplet on the α–bis-PCBM containing film was 61.70°, while for PCBM and the controls, the values were 69.40°and 73.46°, respectively, indicating a better wetting of the α–bis-PCBM containing perovskite by the CB compared to the other two samples.[11]

To further examine the crystal structure of the perovskite films, we conducted thin film X-ray diffraction (XRD) measurements for deposited on m-TiO_2/c-TiO_2/FTO substrates (**Figure 2a**). All the samples show the same trigonal perovskite phase with the dominant (111) lattice reflection. The peak at 12.5° arises from the (001) lattice planes of PbI_2. The excess PbI_2 is believed to passivate surface defects, increasing the solar cell performance.[29,30] By taking the full width at half maximum (FWHM) of the (111) reflection, we calculate the crystallite size using Scherrer's equation. Their size increases from 38 nm to 49 nm and 67 nm for the control, PCBM and α-bis-PCBM respectively. We attribute the larger crystal sizes to the templating effect of PCBM or α-bis-PCBM on the crystal growth. These observations indicate that α-bis-PCBM -containing perovskite film has a higher crystal quality. We ascribe the high-quality crystallization as one of the main factors for improved device performance.[31-33]

We exposed unsealed films of pristine, PCBM and α-bis-PCBM - containing perovskite film to ambient environments, and periodically recorded their film X-ray diffraction patterns. The decomposition of perovskite in moist air is known to lead to the formation of PbI_2 phase.[34] In **Figure 2a**, the ratio of PbI_2 (12.5°)/ perovskite (13.8°) of pristine control perovskite increases faster than that of PCBM-containing and α-bis-PCBM -containing perovskite film after 40 days. The α-bis-PCBM-containing perovskite film turned out to be the most stable one in this test environment, which can also be seen from the **Figure 2b**. The color of α-bis-PCBM -containing perovskite film was persistent whereas that of the PCBM-containing and pristine control perovskite film faded from black to yellow. **Figure 2c** shows measurements of the contact angle formed by a deionized water droplet with the pristine control, PCBM and α-bis-PCBM -containing perovskite film. The derived contact angles are 71.56°, 63.30° and 47.10° for the α-bis-PCBM, PCBM-containing film and the pristine control respectively. This trend reflects a strong increase in hydrophobicity of the perovskite upon incorporation of the

α–bis-PCBM providing a rational for its greatly enhanced stability against degradation in humid air.

To understand the large enhancement of PCE and external quantum efficiencies in the mixed perovskite solar cells, we performed photoluminescence (PL) characterizations for the corresponding samples on glass substrate. The introduction of an electron-accepting fullerene into perovskite layer should largely quench the PL for ensuring fast electron-collection efficiency in complete devices.[18,35] As shown in **Figure 3a**, the sample of PCBM-containing perovskite layer quenches the PL only by 54%, while the α-bis-PCBM -containing sample quenches the PL by 79%. The increased PL quenching yield of the α–bis-PCBM -containing sample indicates an improved electron transfer from perovskite to α–bis-PCBM. The time-resolved PL decay measurement showed similar results and the stretched exponential decay lifetimes are obtained by fitting the data with biexponential decay function (**Figure 3b**). [36] These results are in agreement with the improved IPCE plateau and larger J_{SC} values of the α–bis-PCBM -containing perovskite based cells.[35]

We fabricate perovskite solar cells with the structure of Au/SpiroOMeTAD/ perovskite /mesoporous TiO_2/compact TiO_2/FTO, the cross sectional scanning electron microscopy (SEM) image of which is shown in **Figure 4a**. **Figure 4b** shows the J–V characteristics of pristine perovskite, PCBM and α-bis-PCBM -containing perovskite layer-based PSCs under AM 1.5G illumination with the light intensity of 100 mW cm^{-2}. The key cell parameters are summarized in **Table S1**. The control device based on pristine perovskite has a short-circuit current density (J_{sc}) of 23.32 mA cm^{-2}, an open-circuit voltage (V_{oc}) of 1.09 V, a fill factor (FF) of 0.71, and a resulting PCE of 18.8 %, which are comparable with previously reported values.[5] In contrast, PCBM and α–bis-PCBM -containing perovskite-based devices exhibit significant improvements in both Jsc ,Voc and FF. The PCBM-containing perovskite-based solar cells present the best performance with PCE of 19.9 %, Jsc of 23.73 mA cm^{-2}, Voc of

1.11 V, and FF of 0.73, while the α–bis-PCBM -containing perovskite-based solar cells present the best performance with PCE of 20.8 %, Jsc of 23.95 mA cm^{-2}, Voc of 1.13 V, and FF of 0.74. As reported, PCBM plays a critical role in improving the quality of the active layer with large grains and fewer grain boundaries, which result in obviously enhanced Jsc and FF.[37,38] In present case, *Jsc* and *FF* were also increased from 23.32 to 23.73 mA cm^{-2} and from 0.71 to 0.73, respectively. By replacing PCBM with α–bis-PCBM, *Jsc* and *FF* were further increased to 23.95 mA cm^{-2} and 0.74, respectively. We ascribed the improvement of *Jsc* based on α-bis-PCBM-containing perovskite mainly to improved photoelectron transport speed [**Figure S5**], higher conductivity, higher mobility [**Table S2**] and no obvious boundaries. The commonly observed hysteresis[39] is virtually negligible in our devices as proven by J-V curves shown in **Figure 4b**. The stabilized power outputs from devices based on pristine perovskite, PCBM and α-bis-PCBM-containing perovskite layer are 18.6 %, 19.7 % and 20.7 % respectively (**Figure 4d**), consistent with the obtained PCE.

The incident photon-to-electron conversion efficiency (IPCE) spectrum of the cells based on the corrosponding perovskite layers are presented in **Figure 4c**. The integrated current densities estimated from the IPCE spectra (21.7 mA cm^{-2}, 22.3 mA cm^{-2} and 22.8 mA cm^{-2} for pristine comtrol, PCBM and α-bis-PCBM-containing perovskite layer based on solar cells, respectively) are in good agreement with the Jsc values obtained from the J-V curves. The reproducibility of the device performance was also evaluated by characterizing about 20 cells. **Figure 3c,d,e,f** shows a histogram of the PCE parameters in these devices which indicates excellent reproducibility.

In addition, degradation of the perovskite solar cells is mainly associated with the decomposition of the perovskite active layer due to corrosion by moisture that can intrude into the perovskite active layer through the degraded top electrode[40,41] and with the leakage current caused by the formation of hot spots in the bulk or at the interface.[42] **Figure 5** and **S6,S7**

shows the stability tests of corresponding perovskite solar cells in ambient environment of 40% relatively humidity without encapsulation, in ambient environment of 40% relative humidity at 65℃ with encapsulation and under continuous full sun illumination and maximum power point tracking in a nitrogen atmosphere at room temperature without encapsulation respectively. Obviously, the α-bis-PCBM-containing perovskite based device presents a better stability than that based on the pristine control perovskite and PCBM-containing perovskite. As shown in **Figure 5a**, the PCE maintained 90.1% of the initial value in the α-bis-PCBM-containing perovskite -based device, whereas it decreased to 45.4% and 72.6% of the initial value in the pristine control perovskite and PCBM-containing perovskite based solar cells after 44 days. The devices with α-bis-PCBM -containing perovskite layer exhibited negligible degradation (less than 10%) upon exposure to air for 44 days at 65℃ shown in **Figure 5b**. Moreover, preliminary test in **Figure S7** shows that the α-bis-PCBM-containing perovskite based device is more resistant to heat stress than the device based on PCBM-containing and pristine control perovskite at 85℃. **Figure 5c** indicates that there is only 4% efficiency drop after 600 h under continuous full sun illumination and maximum power point tracking for α-bis-PCBM -containing perovskite solar cell.We ascribed the improvement of stability based on α-bis-PCBM-containing perovskite mainly to the presence of less holes pinholes in the spiro-OMeTAD layer (**Figure S9**) , lager grain size and no obvious boundaries.[8,9,43,44]As a result, the α-bis-PCBM-containing perovskite based device showed a much stronger resistance to degradation over longer time periods than the other two corresponding devices, as indicated in **Figure 5** and **S6-S8**.

In conclusion, We have demonstrated PSCs with simultaneously improved device performance and stability based on a one-step solution-processable strategy by a facile α-bis-PCBM-containing perovskite growth method during the device fabrication. The α-bis-PCBM network could resist moisture incursion, thus preventing erosion of the interfaces and

passivating the voids or pinholes generated in the bulk active layer. The introduction of α-bis-PCBM can also address the issue of low electron extraction efficiency, enhance the crystallization of perovskites, and improve the stability of the PSCs. The promising approach provides a simple route for the fabrication of highly efficient and stable bulk heterojunction perovskite solar cells.

Supporting Information

Supporting Information is available from the Wiley Online Library or from the author.

Acknowledgements:

We thank Dr. Giordano Fabrizio (LPI) in help with the IMPS test and Mr.Linfeng Pan(LSPM) for hall effect test.FZ thanks the China Scholarship Council for funding. SRW and XGL thank the National Natural Science Foundation of China (21676188) and Key Projects in Natural Science Foundation of Tianjin (16JCZDJC37100) for support. JL acknowledges financial support by Marie Curie Fellowship from the European Union's Seventh Framework Programme (No. 291771) and the SNF-Nanotera RTD Project SYNERGY. MG. And SMZ thanks the King Abdulaziz City for Science and Technology (KACST) for financial support. Financial support from the Swiss National Science Foundation (SNSF), the NRP 70 "Energy Turnaround", CCEM-CH in the 9th call proposal 906: CONNECT PV, the European Union's Horizon 2020 research and innovation programme under the grant agreement No 687008 (GOTSolar) as well as from SNF-NanoTera and Swiss Federal Office of Energy (SYNERGY) is also gratefully acknowledged. The information and views set out in this article are those of the author(s) and do not necessarily reflect the official opinion of the European Union. Neither the European Union institutions and bodies nor any person acting on their behalf may be held responsible for the use which may be made of the information contained herein.

Received: ((will be filled in by the editorial staff))
Revised: ((will be filled in by the editorial staff))
Published online: ((will be filled in by the editorial staff))

[1] F. Zhang, S.R. Wang, X.G. Li , Y. Xiao, *Curr. Nanosci*. **2016**, 12, 137-156..

[2] H.Zhou, Q.Chen, G.Li, S.Luo, T.Song, H.-S.Duan, Z.Hong, J.You, Y.Liu, Y.Yang, *Science*,**2014**, 345, 542−546..

[3] H. S. Jung, N.-G.Park, *Small*,**2015**, 11, 10−25.

[4] W. S. Yang, J. H. Noh, N. J. Jeon, Y. C. Kim, S. Ryu, J. Seo ,S. I. Seok, *Science*, **2015**, 348, 1234-1237.

[5]D.Q.Bi,W.Tress,M.I.Dar, P.Gao, J.S.Luo, C.Renevier, K.Schenk,A.Abate, F.Giordano, J.C.Baena,J.Decoppet,S.M.Zakeeruddin,M.K.Nazeeruddin, M.Grätzel ,A.Hagfeldt, *Sci. Adv.* **2016**,2,e1501170.

[6]T.A.Berhe, W.N.Su, C.H.Chen, C.J.Pan, J.H.Cheng, H.M.Chen, M.C. Tsai, L.Y.Chen, A.A.Dubaleb, B.J.Hwang, *Energy Environ. Sci*. **2016**, 9, 323–356

[7] NREL.Best Research-Cell Efficiencies, http://www.nrel.gov/ncpv/images/effi ciency_chart.jpg . (Dec **2016**)

[8] F.Zhang, C.Y.Yi, P.Wei, X.D. Bi, J.S. Luo,G.Jacopin, S.R. Wang, X.G. Li , Y.Xiao , S. M. Zakeeruddin, M. Grätzel , *Adv. Energy Mater.* **2016**, 6,1600401.

[9] C.H. Chiang, C.G.Wu, *ChemSusChem*, **2016**, 9,.2666–2672.

[10] C.Y. Chang, W.K. Huang, Y.C. Chang, *Chem. Mater*,**2016**, 28 (17), 6305–6312 .

[11]M.Moriya,D.Hirotani,T.Ohta,Y.Ogomi,Q.Shen,T.S.Ripolles,K.Yoshino,T.Toyoda,T.Minemoto,S.Hayase, *ChemSusChem*, **2016**, 9,2634–2639.

[12] M. D. McGehee, *Nat. Mater.*, **2014**, 13, 845.

[13] T. A.Berhe, W.N.Su, C.H.Chen, C.J.Pan, J.-H.Cheng,H.M.Chen,M.C.Tsai, L.Y.Chen, A. A.Dubale, B.J.Hwang,*Energy Environ. Sci.* **2016**, 9, 323−356.

[14] H.Tiep, Z.Ku,H. J. Fan, *Adv. Energy Mater.* **2016**, 6,1501420.

[15] D.Q. Bi, C.Y.Yi, J.S.Luo, J.D. Décoppet, F.Zhang, S.M. Zakeeruddin, X. Li, A.Hagfeldt , M.Grätzel, *Nature Energy* ,**2016**, 1,16142.

[16] M.Salado,F. J.Ramos,V.M. Manzanares,P.Gao,M.K.Nazeeruddin,P.J. Dyson,S. Ahmad, *ChemSusChem*, **2016**, 9,2708–2714

[17]C. Liu, K. Wang, P. C. Du, C. Yi, T. Y. Meng ,X. Gong, *Adv.Energy Mater.*, **2015**, 5, 1402024.

[18]K. Wang, C. Liu, P. C. Du, J. Zheng,X. Gong, *Energy Environ. Sci.*, **2015**, 8, 1245-1255.

[19] C. H. Chiang, C. G. Wu, *Nat. Photonics*, **2016**, 10, 196.

[20] J.J.Chang,Z.H.Lin,H.Zhu,F.H. Isikgor,Q.H.Xu,C.F.Zhang,Y.HaoJ.Y.Ouyang, *J. Mater. Chem. A*, **2016**, 4,16546-16552.

[21]M.Saliba1,T.Matsui1,K.Domanski1,J.Y.Seo,A.Ummadisingu,S.M.Zakeeruddin,J-P.P. Correa-Baena,W.R. Tress,A,AbateA.Hagfeldt,M. Grätzel, *Science,***2016**, DOI: 10.1126/science.aah5557.

[22] M.Lenes,S.W.. Shelton,A.B.. Sieval,D.F. Kronholm,J.C. Hummelen,P.W. M. Blom, *Adv. Funct. Mater*. **2009**,19, 3002-3007.

[23] Y.Matsuo, *Chem. Lett*. **2012**,41, 754-759.

[24] R.K.M.Bouwer, G.J.A.H.Wetzelaer, P.W.M. Blom, J.C.Hummelen, *J. Mater. Chem.* **2012**,22, 15412-15417.

[25] Y. Kim, C.H.Cho, H.Kang, K.H.Kim, S.Park, T.E. Kang, K.Park, B.J. Kim, *Solar Energy Materials and Solar Cells*, **2015**, 141, 87-92.

[26] M. Xiao, F. Huang, W. Huang, Y. Dkhissi, Y. Zhu,J. Etheridge, A. Gray-Weale, U. Bach, Y. B. Cheng ,L. Spiccia, *Angew. Chem.*, **2014**, 126, 10056–10061.

[27]J. Xu, A. Buin, A. H. Ip, W. Li, O. Voznyy, R. Comin, M. Yuan,S. Jeon, Z. Ning, J. J. McDowell, P. Kanjaaboos, J. P. Sun,X. Lan, L. N. Quan, D. H. Kim, I. G. Hill, P. Maksymovych ,E. H. Sargent, *Nat. Commun.*, **2015**, 6, 7081.

[28] C.Li, J.Sleppy, N. Dhasmana, M.Soliman, L.Tetardd,J, Thomas, *J. Mater. Chem. A*, **2016**, 4, 11648–11655.

[29]T.Y. Zhang, N.J.Guo, G.Li, X.F. Qian, Y.X. Zhao, *Nano Energy*, **2016**,26,50-56.

[30]Y.Tidhar, E.Edri, H.Weissman, D.Zohar, G.Hodes, D. Cahen, B.Rybtchinski, S. Kirmayer, *J. Am. Chem. Soc.***2014**, 136, 13249-13256.

[31] M. Li, Z. K. Wang, Y. G. Yang, Y. Hu, S. L. Feng, J. M. Wang,X. Y. Gao, L. S. Liao, *Adv. Energy Mater.*, **2016**, 1601156.

[32]Z. K. Wang, M. Li, Y. G. Yang, Y. Hu, H. Ma, X. Y. Gao,L. S. Liao, *Adv. Mater.*, **2016**, 28, 6695.

[33] Z. K. Wang, X. Gong, M. Li, Y. Hu, J. M. Wang, H. Ma ,L. S. Liao, *ACS Nano*, **2016**, 10, 5479.

[34] D.Q.Bi,P.Gao,R.Scopelliti,E. Oveisi,J.S. Luo,M. Grätzel,A.Hagfeldt,M.K. Nazeeruddin, *Adv. Mater.***2016**,28, 2910–2915.

[35]Y.Z.Wu,X.D.Yang,W.Chen,Y.F.Yue,M.L.Cai, F.X. Xie,E.B.Bi,A.Islam,L.Y.Han, *Nature Energy*, **2016**, 1,16148.

[36] F. Zhang, X. Liu, C. Yi, D. Bi, J.Luo, S. Wang, X. Li, Y.Xiao, S. Zakeeruddin, M. Grätzel, *ChemSusChem*, **2016**,9, 2578–2585.

[37] M. Li, Y.H. Chao, T.Kang, Z.K.Wang,Y.G. Yang,S.L. Feng, Y. Hu, X.Yu Gao, L.S.Liao,C.S. Hsu, *J. Mater. Chem. A,* **2016**, 4, 15088-15094.

[38]D. X. Yuan, A. Gorka, M. F. Xu, Z. K. Wang , L. S. Liao,*Phys. Chem. Chem. Phys.*, **2015**, 17, 19745.

[39] Y.Shao, Z.Xiao, C.Bi, Y.Yuan, J.S.Huang, *Nat. Commun*.**2014**, 5, 5784.

[40]P. W. Liang, C. Y. Liao, C. C. Chueh, F. Zuo, S. T. Williams,X. K. Xin, J. Lin ,A. K. Y. Jen, *Adv. Mater.*, **2014**, 26, 3748.

[41]J. M. Frost, K. T. Butler, F. Brivio, C. H. Hendon,M. V. Schilfgaarde, A. Walsh, *Nano Lett.*, **2014**, 14, 2584.

[42]R. Steim, S. A. Choulis, P. Schilinsky, U. Lemmer,C. J. Brabec, *Appl. Phys. Lett.*, **2009**, 94, 043304.

[43] Y.Yuan,J.S. Huang, *Acc.Chem. Res*. **2016**, 49, 286−293.

[44]H.Back, G.Kim, J.Kim, J.Kong,T.K. Kim, H. Kang, H. Kim,J.Lee, S.Lee, K.Lee, *Energy Environ. Sci.* **2016**, 9, 1258−1263.

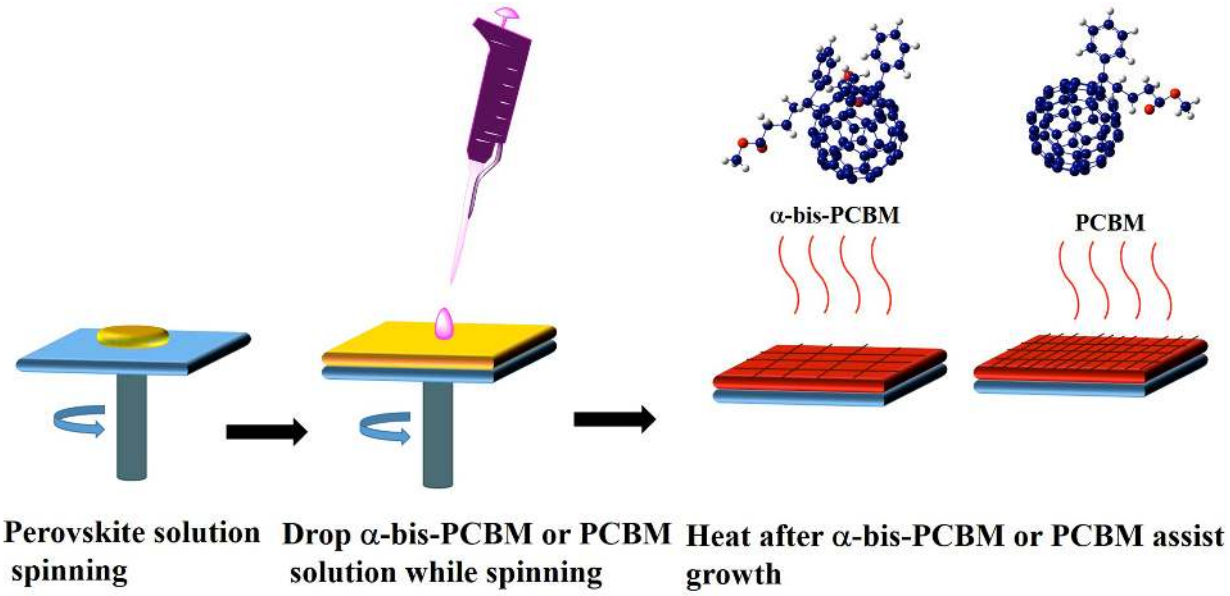

Figure 1 Schematic diagram of the α−bis-PCBM or PCBM-containing growth resulting in a perovskite- α−bis-PCBM or PCBM hybrid structure process flow for devices.

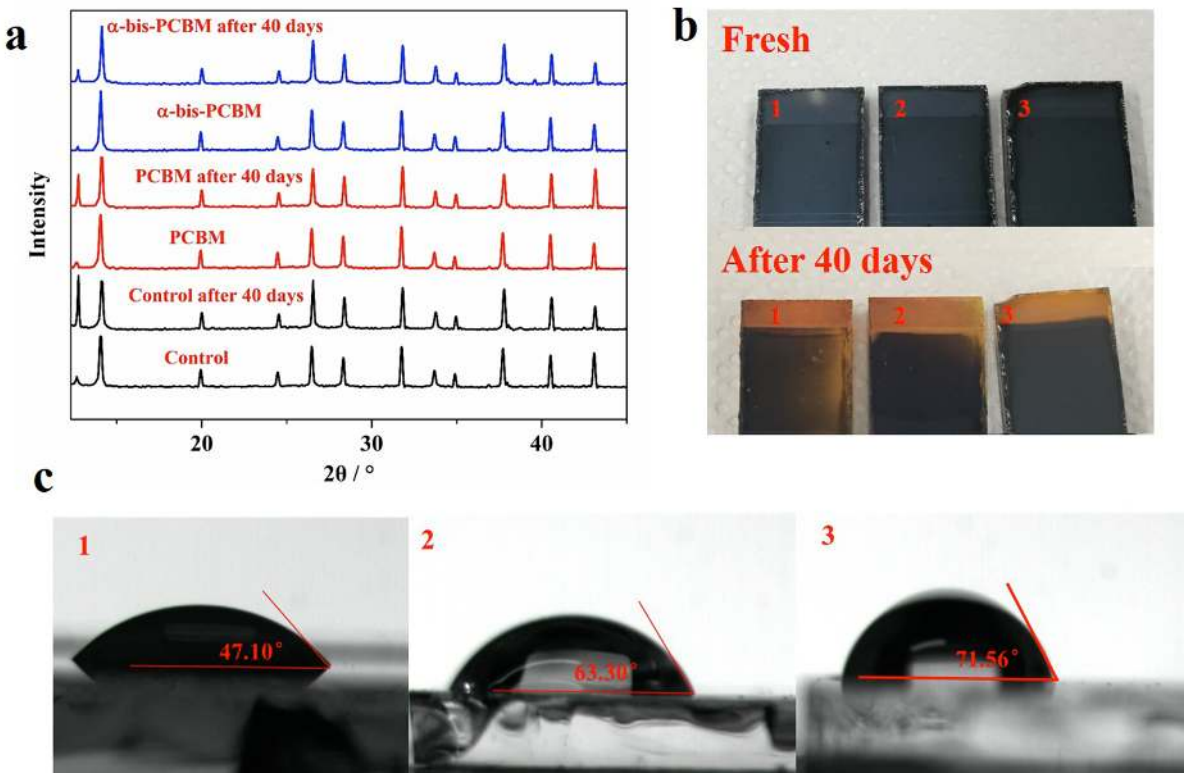

Figure 2 a) XRD patterns of corresponding films on meso-TiO_2/compact TiO_2/FTO substrate, which were exposed to ambient 40% relative humidity. b) The pictures of the corresponding films before and after aging to ambient 40% relative humidity. c) The contact angles between perovskite films and water: 1, Control; 2, PCBM; 3, α–bis-PCBM.

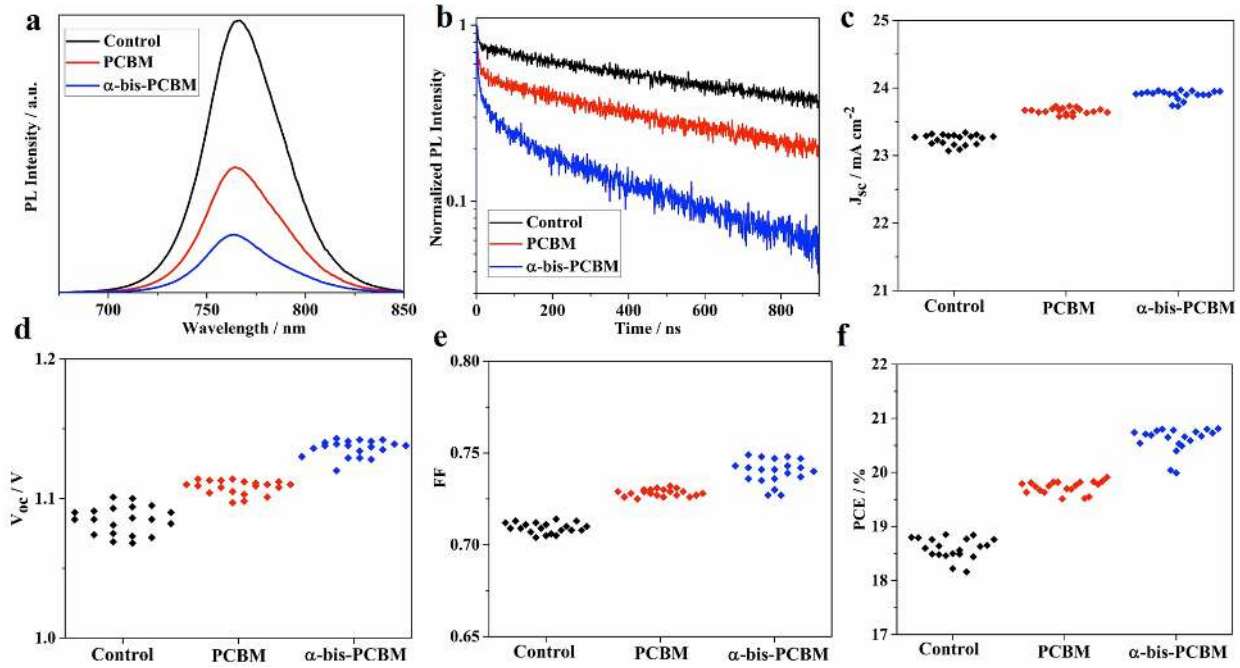

Figure 3 a) PL spectra,b)TRPL spectra of corresponding films on glass substrate. c,d,e,f) Photovoltaic metrics of devices based on corresponding perovskite layers.

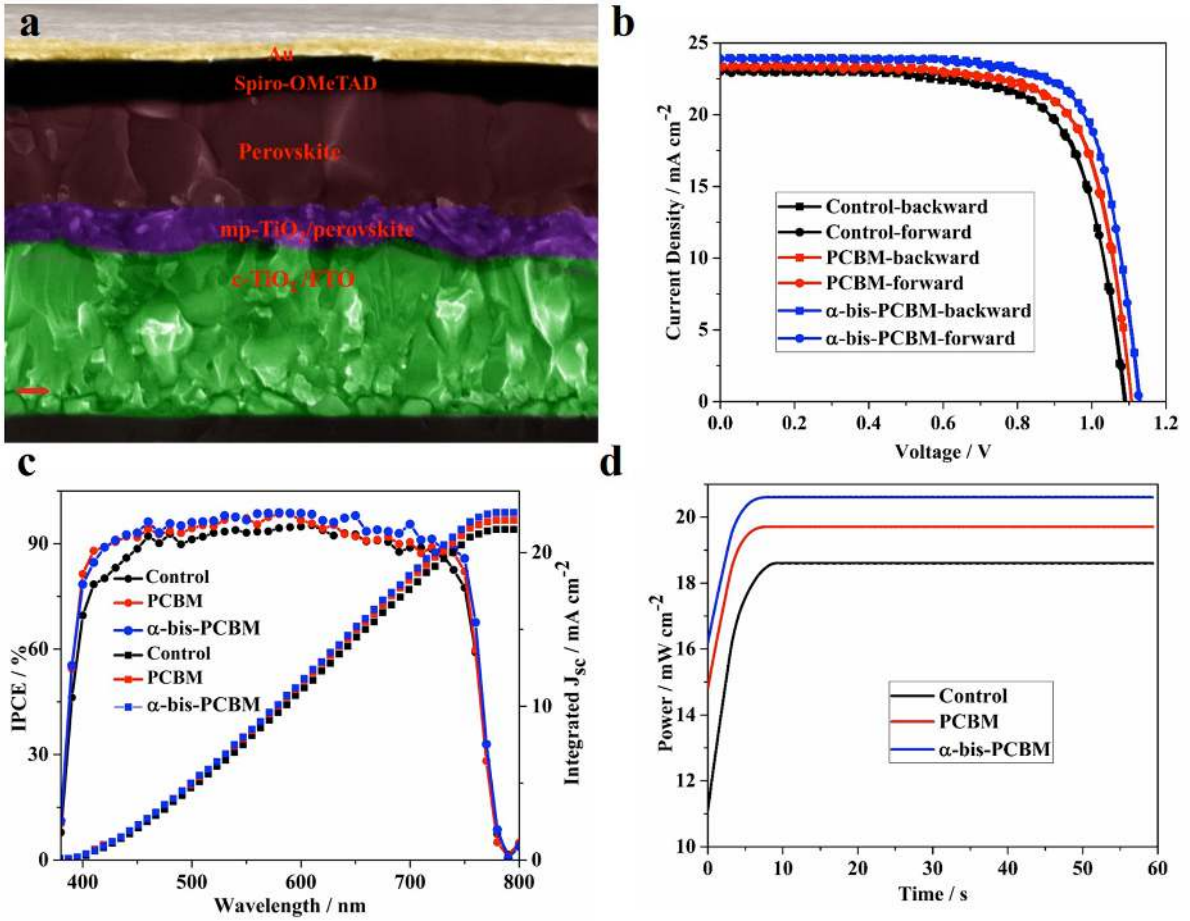

Figure 4 a) Cross-sectional SEM image of the device based on Bis-PCBM.The scale bar is 100 nm. b) Current-voltage hysteresis curves of perovskite solar cells comprising champion devices measured starting with backward scan and continuing with forward scan. c) IPCE spectra and integrated current curves of the corresponding devices. d) The stabilized power output of the corresponding devices.

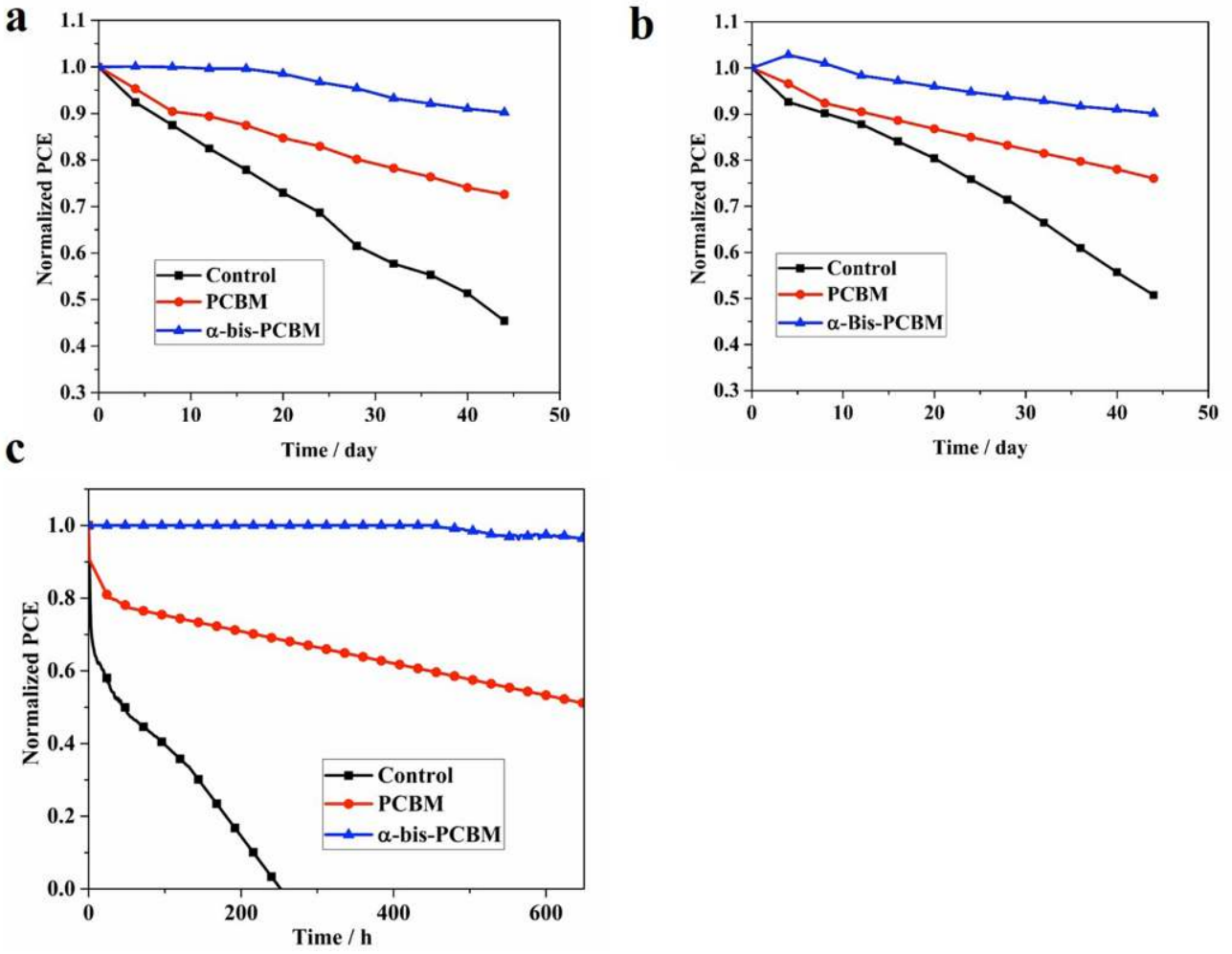

Figure 5 The stability of corresponding perovskite solar cells in ambient environment of 40% relatively humidity. a) Under dark without any encapsulation at room temperature. b) Under dark with encapsulation at 65℃. c) The stability of corresponding perovskite solar cells under continuous full sun illumination and maximum power point tracking in a nitrogen atmosphere at room temperature .

A significantly improved performance for mixed perovskite solar cells by a facile α–bis-PCBM -containing perovskite growth method during the device fabrication was reported. The newly developed PSC exhibited an enhanced PCE of 20.8 % along with enhanced stability under heat and illumination.

Keyword: stability; PCBM; perovskite solar cell

Fei Zhang, Wenda Shi, Jingshan Luo, Norman Pellet , Chenyi Yi, Xiong Li, Xiaoming Zhao, T. John. S. Dennis, Xianggao Li, Shirong Wang*, Shaik Mohammed Zakeeruddin, Dongqin Bi*, Michael Grätzel**

Isomer-pure bis-PCBM assisted crystal engineering of perovskite solar cells showing excellent efficiency and stability

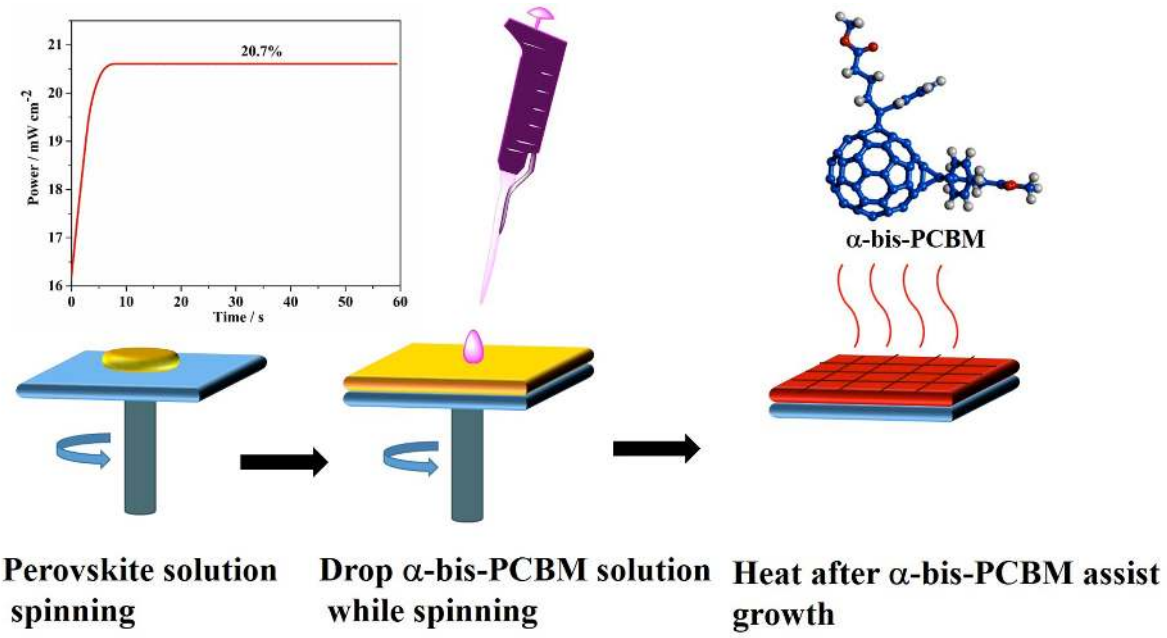

Supporting Information

Isomer-pure bis-PCBM assisted crystal engineering of perovskite solar cells showing excellent efficiency and stability

Fei Zhang, Wenda Shi, Jingshan Luo, Norman Pellet , Chenyi Yi, Xiong Li, Xiaoming Zhao, T. John. S. Dennis, Xianggao Li, Shirong Wang*, Shaik Mohammed Zakeeruddin, Dongqin Bi*, Michael Grätzel**

Experimental

Instrument and Measurements: UV-vis spectra of the HTMs in tetrahydrofuran (THF) solutions (1×10^{-5} mol L^{-1}) was recorded with Thermo Evolution 300 UV-Vis spectrometer (Thermo Electron, USA) in the 200-800 nm wavelength range at room temperature. Surface morphology of the TiO_2/perovskite/HTM/Au film was obtained by using a scanning electron microscope (SEM, ZEISS Merlin). Photoluminescence (PL) spectra were recorded with Fluorolog-Horiba fluorometer. The XRD patterns were acquired with a Bruker D8 Discover diffractometer in Bragg–Brentano mode, using Cu Kα radiation (1.540598 Å) and a Ni β-filter. Spectra were acquired with a linear silicon strip "Lynx Eye" detector from 2θ = 10°– 60° at a scan rate of 2° min^{-1}, step width of 0.02°, and a source slit width of 1 mm. A baseline correction was applied to all X-Ray thin film diffractograms to compensate for the broad feature arising from the glass.

Device fabrication: Devices were prepared on conductive fluorine-doped tin oxide (FTO) coated glass substrates. The substrates were cleaned extensively by deionized water, acetone and isopropanol. A compact titanium dioxide (TiO_2) layer of about 40 nm was deposited by spray pyrolysis of 7 ml 2-propanol solution containing 0.6 mL titanium diisopropoxide bis(acetylacetonate) solution (75% in 2-propanol, Sigma-Aldrich) and 0.4 mL acetylacetone at 450 ℃ in air. On top of this layer, mesoporous titanium dioxide was formed by spin-

coating 30 nm sized nanoparticles (Dyesol 30NRD, Dyesol) diluted in ethanol (1:6 *w*/*w*) at 4500 r.p.m. for 15 s. The $[(FAI)_{0.81}(PbI_2)_{0.85}(MABr)_{0.15}(PbBr_2)_{0.15}]$ precursor solution was prepared in a glovebox from a 1.35M Pb^{2+}(PbI_2 and $PbBr_2$) in the mixed solvent of DMF and DMSO, the volume ratio of DMF/DMSO is 4:1. The spin-coating procedure was performed by 2000 rpm for 10 s followed with 6000 rpm for 30 s. At 15 s before the last spin-coating step, 100 ml of α–bis-PCBM or PCBM solution with 0.4 mg/mL from chlorobenzene was pipetted onto the substrate. Thereafter, the substrate was put onto a hotplate for 1 hour at 100°C. Subsequently, the HTM were deposited on the top of perovskite by spin coating at 4000 r.p.m. for 15 s. The spiro-OMeTAD solutions were prepared dissolving the spiro-OMeTAD in 1 ml chlorobenzene at concentration of dissolving the spiro-OMeTAD in chlorobenzene at a concentration of 60 mM, with the addition of 30 mM bis(trifluoromethanesulfonyl)imide from a stock solution in acetonitrile), 200 mM of tert-butylpyridine. The devices were finalized by thermal evaporation of 80 nm gold.

J-V Characterization: The J-V characteristics of the devices were measured under 100mW/cm^2 conditions using a 450 W Xenon lamp (Oriel), as a light source, equipped with a Schott K113 Tempax sunlight filter (Praezisions Glas & Optik GmbH) to match the emission spectra to the AM1.5G standard in the region of 350-750 nm. The current–voltage characteristics of the devices were obtained by applying external potential bias to the cell while recording the generated photocurrent 3 using a Keithley (Model 2400) digital source meter. The J–V curves of all devices were measured by masking the active area with a metal mask of area 0.16 cm^2.

IPCE: The incident photon to current conversion efficiency of the devices was measured by focusing light from the 300W Xenon lamp (ILC Technology, U.S.A.) through a Gemini-180 double monochromator (Jobin Yvon Ltd., U.K.). The monochromatic light was chopped at 3 Hz before impinging onto the photovoltaic cell. The monochromator was incremented through the visible spectrum to generate the IPCE dependence on wavelength.

Long term light soaking test: Stability measurements were performed with a Biologic MPG2 potentiostat under a full AM 1.5 Sun-equivalent white LED lamp. The devices were measured with a maximum power point (MPP) tracking routine under continuous illumination (and nitrogen). The MPP was updated every 10 s by a standard perturb and observe method. Every 1 minutes a JV curve was recorded in order to track the evolution of individual JV parameters.

The purification of Bis-PCBM :The individual isomers were separated from each other using a Japan Analytical Industries LC908 peak recycling high performance liquid chromatography (″HPLC″) machine using an absorption detector operating at 312 nm. Initially, 1.0 g of an as-produced isomer mixture of bis-[60]PCBM was dissolved in 700 ml of HPLC-grade toluene and then filtered through a 0.45 μm PTFE membrane. For Stage 1, the entire sample was processed through about 250 separate runs, whereby for each run 3.0 ml of the solution injections onto a Waters 5 μm silica column (19 mm i.d. × 150 mm) with a flow rate of 18 ml min^{-1}, after which elution continued with pure toluene in normal single-pass mode. Subsequent stages were carried out in peak-recycling mode using fractions from the preceding stages. During these subsequent stages, in addition to the abovementioned silica column, multi-columns were used as appropriate. The most abundant isomer with addition position [1,9] and [30,31] was purified out, and the molecular structure is shown below.

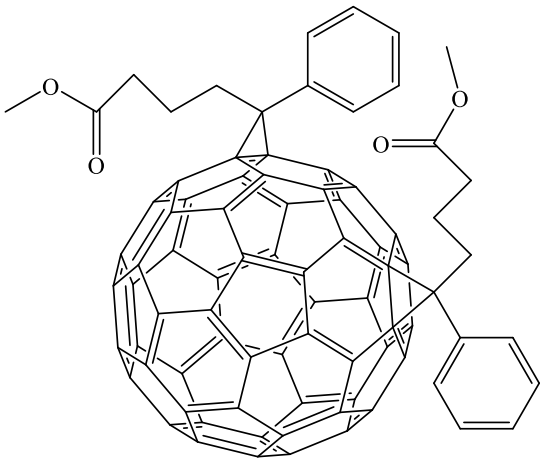

Figure S1 Molecular structures of monomer α-bis-PCBM.

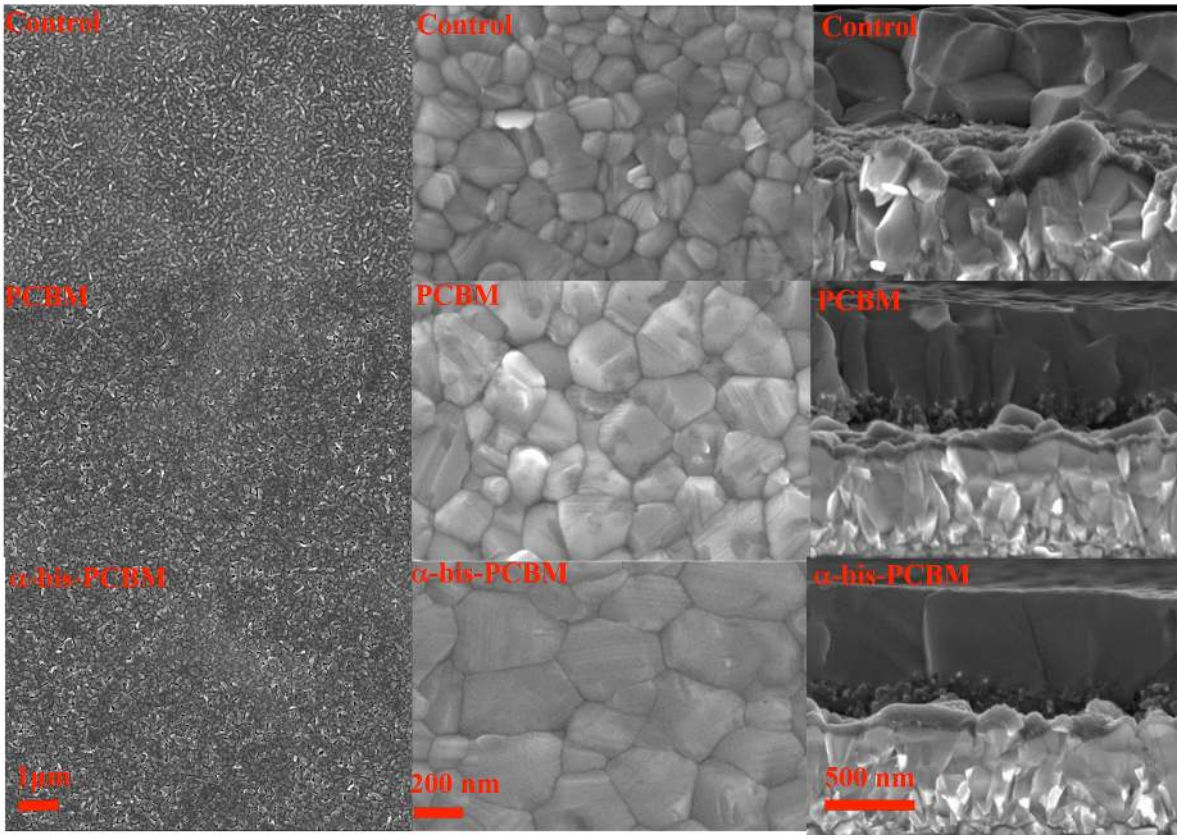

Figure S2 Scanning electron microscopy images. Top (left and middle colum) and cross sectional (right column) SEM of corresponding perovskite films. The left column of images are perovskite film before annealing, while the middle ones and the right ones are films after annealing.

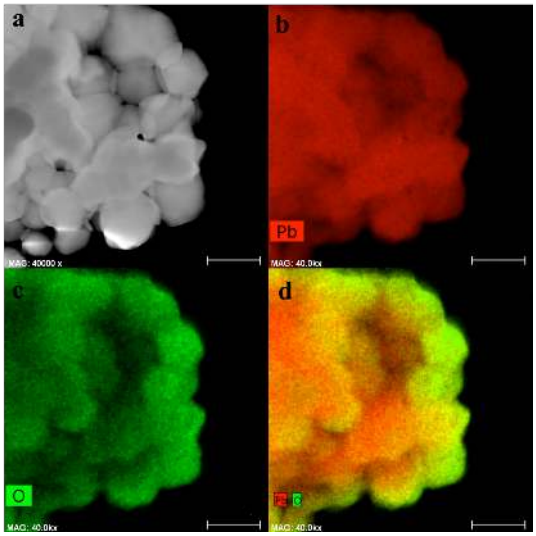

Figure S3 High-angle annular dark-field scanning transmission electron microscopy (HAADF-STEM) and scanning transmission electron microscopy coupled with energy dispersive X-ray spectroscopy (STEM-EDS) of the corresponding perovskite.The scale is 1μm.

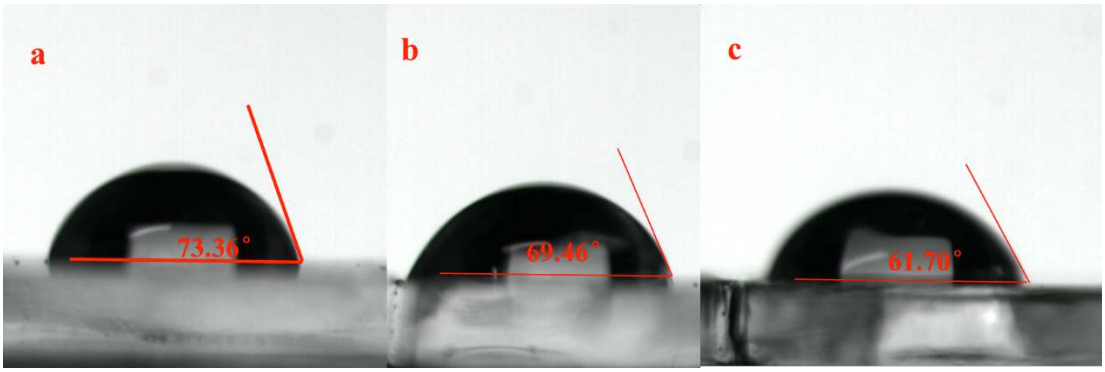

Figure S4 The contact angles between perovskite films and chlorobenzene, (a) control; (b) PCBM; (c) α–bis-PCBM

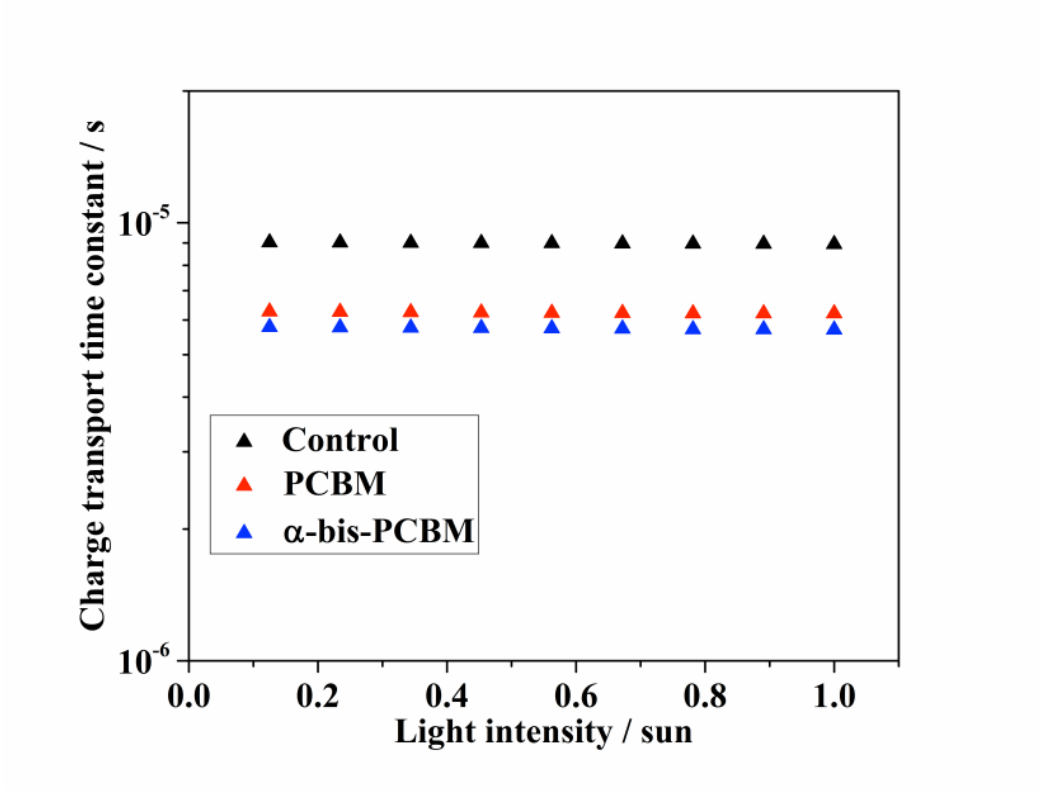

Figure S5 Charge transport lifetime as function of the light intensity for corresponding perovskite solar cells extracted by intensity-modulated photocurrent spectroscopy

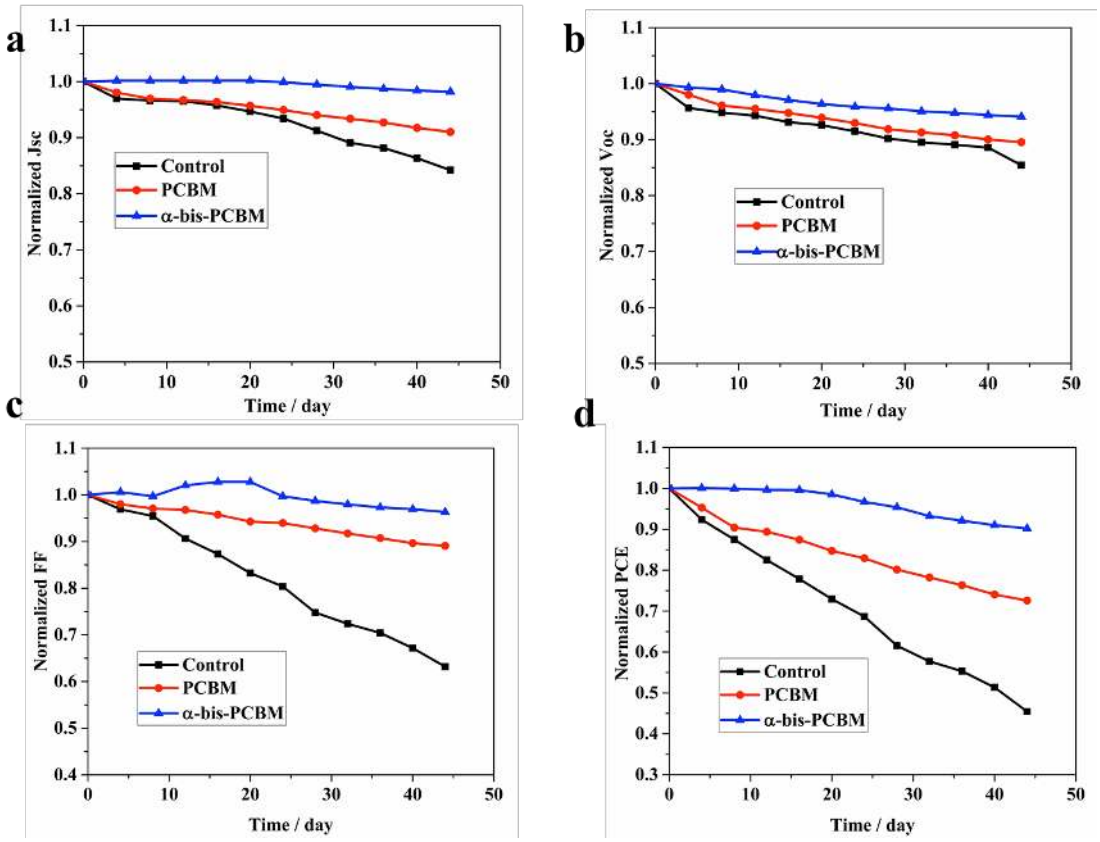

Figure S6 The stability of corresponding perovskite solar cells without any encapsulation in ambient environment of 40% relative humidity.

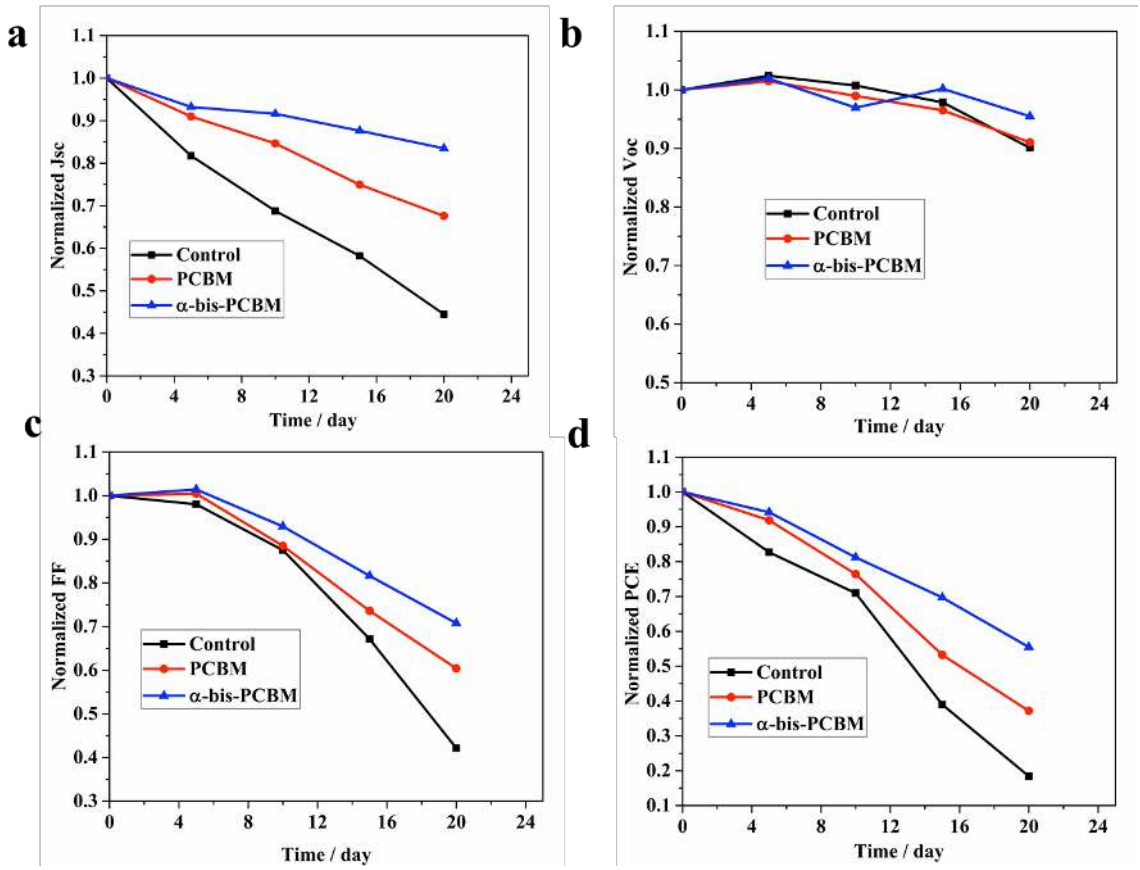

Figure S7 The stability of perovskite solar cells in ambient air without encapsulation at 85 ℃.

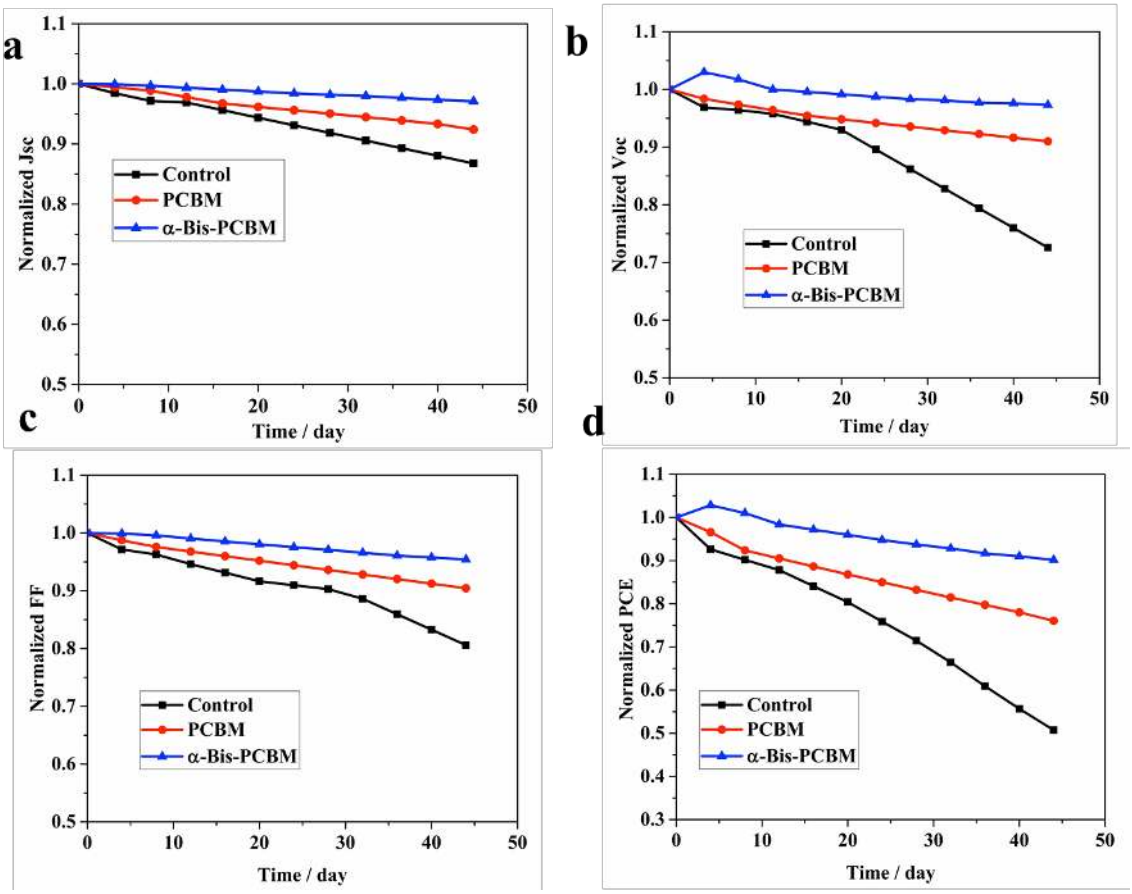

Figure S8 The stability of corresponding perovskite solar cells with encapsulation at 65℃ in ambient environment of 40% relative humidity.

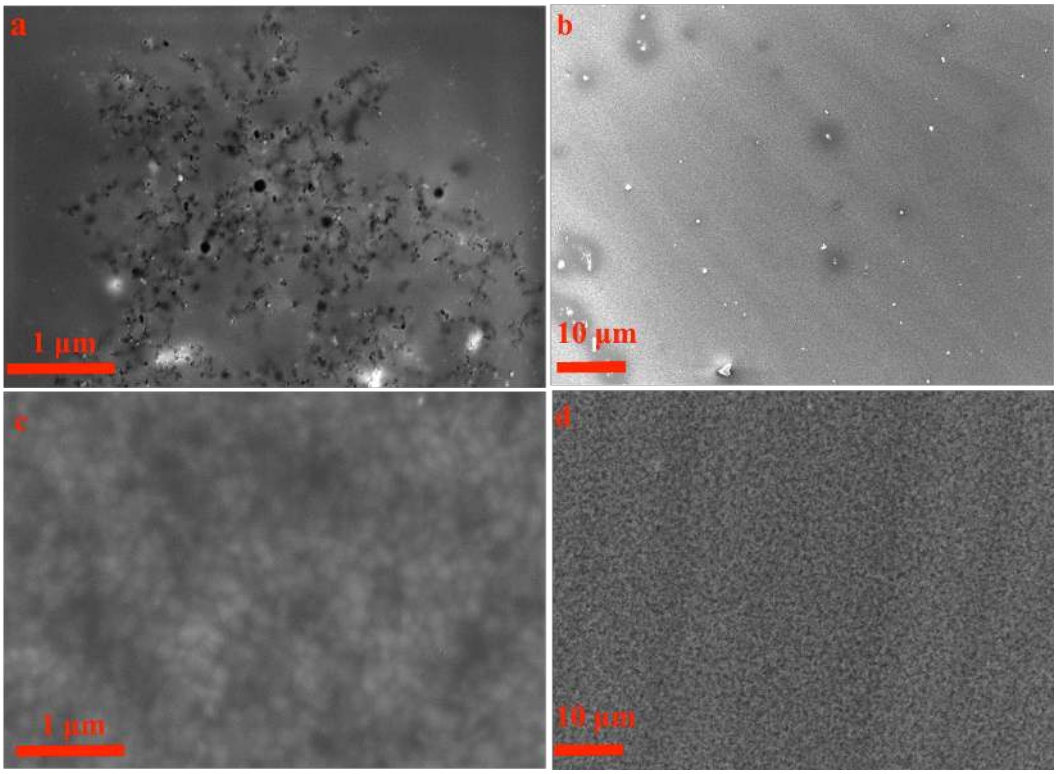

Figure S9 Surface view SEM images of spiro-OMeTAD on (a,b) perovskite; (c,d) α–bis-PCBM /perovskite.The scale bar of a, c is 1 μm and b, d is 10 μm.

Table S1 Performance parameters of corrosponding perovskite-based solar cells under different scan directions with a bias step of 5 mV.

Sample	V_{oc} (V)	J_{sc} (mA cm^{-2})	*FF*	PCE (%)
Control （backward）	1.09	23.32	0.71	18.8
Control （forward）	1.09	23.30	0.71	18.8
PCBM （backward）	1.11	23.73	0.73	19.9
PCBM （forward）	1.11	23.59	0.73	19.9
α-bis-PCBM （backward）	1.13	23.95	0.74	20.8
α-bis-PCBM （forward）	1.12	23.91	0.75	20.8

Table S2 The conductivity and mobility of pure perovskite (Control) and PCBM or α-bis-PCBM containing perovskite film from the hall effect measurment test.

Sample	Conductivity ($S\ cm^{-1}$)	Mobility $cm^2\ Vs^{-1}$
Control	$1.34*10^{-6}$	3.898
PCBM	$5.74*10^{-6}$	6.918
α-bis-PCBM	$2.16*10^{-5}$	62.30